ARPHA Proceedings

Proceedings CAUSummit 2026, 0408-0417
doi: 10.3897/ap.12.e0408

11th Anniversary
World Summit: Civil Engineering-Architecture-Urban Planning Congress

Algorithmic Approach for Optimization of The Direction of Maximum Dispersion and The Orientation of The Error Ellipse with Respect to The Type and Weights of Measurements in Geodetic Networks

Tamara Ilieva [1, a)], Pavel Pavlov [1]

[1] *University of Architecture, Civil Engineering and Geodesy, 1, Hristo Smirnenski Blvd. Rectorate building, 4th fl. Office room 411, Sofia, Bulgaria*

[a)] Corresponding author: ilieva_fgs@uacg.bg

Abstract. The accuracy of determining the positions of points in geodetic networks is described by the error ellipse, which results from the bivariate normal distribution of coordinates. The influence of the type and weights of measurements on the shape and orientation of the ellipse is of essential importance in combined angular and distance measurements, which are widely used in practice. In this context, determining the ellipse's orientation relative to the direction of maximum dispersion is key to the analysis and management of accuracy. In this study, an algorithmic approach is proposed for determining the orientation of the ellipse through analysis of the variance-covariance structure and transformation to the principal axes, which allows unambiguous identification of the direction of maximum dispersion. On this basis, an approach for optimizing the weights in geodetic measurements has been developed, and it has been shown that the appropriate balance between angular and distance measurements allows control over the shape and orientation of the error ellipse and leads to improved accuracy in predefined directions. The scientific contribution of the study consists of integrating the weights of the measurements with the orientation of the error ellipse and the direction of maximum dispersion in a single framework. The proposed approach can be applied in the optimization of schemes for performing geodetic measurements and in the design of networks with predefined accuracy requirements.

Keywords: Error ellipse; maximum dispersion; covariance analysis; weight optimization; angular and distance geodetic measurements; geodetic networks

© 2026 Tamara Ilieva, Pavel Pavlov
This is an open access article distributed under the terms of the Creative Commons Attribution License (CC BY 4.0), which permits unrestricted use, distribution, and reproduction in any medium, provided the original author and source are credited.
Published by CAUSummit and peer-reviewed under the responsibility of "World Summit: Civil Engineering-Architecture-Urban Planning Congress - CAUSummit-2026".

INTRODUCTION

The determination of point-position accuracy is a fundamental task in geodesy and engineering surveying. Currently, the geodetic networks must satisfy the increasing requirements in applications such as engineering construction, deformation monitoring, transportation infrastructure, and cadastral surveying. The resulting positional accuracy is dependent on the combined effects of network geometry, observation precision, the adopted stochastic model, and the adjustment procedure, so the analysis and optimization of positional uncertainty are essential in both network design and accuracy assessment [1–5].

Following least-squares adjustment, the positional uncertainty of an estimated point is represented by the covariance matrix of its coordinates. The variances of the coordinate components together with their covariance define the corresponding error ellipse, whose principal axes characterize the magnitude and directional distribution of the uncertainty. The orientation of the semi-major axis identifies the direction of maximum dispersion [1,2,4,6].

The parameters of the error ellipse are commonly obtained through eigenvalue decomposition of the covariance matrix. The eigenvalues determine the lengths of the principal axes, whereas the associated eigenvectors define their orientation. Equivalent analytical expressions based on covariance-matrix invariants are also widely used in geodetic adjustment theory [2,4,5,7]. These formulations provide a direct relationship between the stochastic properties of the adjusted coordinates and the geometry of the error ellipse [6].

In addition to representing overall positional uncertainty, the covariance matrix allows the accuracy of a point to be evaluated in any predefined direction. Directional accuracy depends on both the dimensions and the orientation of the error ellipse. This characteristic is particularly important in engineering applications in which higher accuracy is required along a specified structural, displacement, or alignment direction. The same principles apply to relative error ellipses, which describe the mutual positional accuracy between pairs of points [7].

The covariance structure of the adjusted coordinates is directly affected by the stochastic model of the observations. Combined geodetic networks generally include angular and distance measurements with different precision characteristics and, consequently, different weights. Distance observations predominantly constrain the radial component of the point position, whereas angular observations primarily influence the transverse component. Changes in their relative weights therefore modify not only the dimensions of the error ellipse but also its covariance term and orientation.

Most previous studies have focused on determining error-ellipse parameters after network adjustment. Considerably less attention has been given to the inverse problem: controlling the direction of maximum dispersion by modifying the stochastic model while preserving the network geometry. In particular, the relationship between the relative weighting of angular and distance observations and the orientation of the error ellipse has not been sufficiently investigated within a unified optimization framework.

This problem is relevant to the preliminary design of engineering-geodetic networks, in which positional and directional accuracy requirements must be assessed before field observations are conducted. Applications include the setting out of structures with prescribed orientation and millimeter-level tolerances [8], the optimization of control-point configurations in bridge and infrastructure networks [9], and deformation-monitoring systems in which covariance analysis and relative error ellipses are used to evaluate the magnitude and direction of structural displacements [10–12].

The present study proposes an algorithmic approach for analyzing and optimizing the orientation of the error ellipse in combined angular–distance geodetic networks. The methodology integrates covariance analysis, eigenvalue decomposition, and systematic modification of observation weights to establish a direct relationship between measurement precision and the directional characteristics of the adjusted coordinates. Two stochastic models are considered: a reference model with equal directional weights and a model incorporating individual instrument- and signal-centering errors.

The proposed procedure enables quantification of the effects of angular and distance observations on the shape and orientation of the error ellipse. It also provides a basis for selecting observation weights that improve accuracy in predefined directions. The approach can therefore support the design and assessment of geodetic networks subject to directional accuracy requirements.

In this study, optimization is understood as the identification of a stochastic model that provides the most favorable uncertainty characteristics with respect to the direction of maximum dispersion and the associated error ellipses. Rather than solving a constrained mathematical optimization problem, the proposed methodology evaluates alternative stochastic models and identifies the weighting strategy that best satisfies the adopted precision criteria.

The main contributions of this study are as follows:

- A unified computational framework linking stochastic modelling, covariance propagation and the direction of maximum dispersion.
- A systematic evaluation of the influence of observation weighting on positional uncertainty and error ellipse characteristics.
- Experimental evidence demonstrating that network geometry predominantly controls the orientation of the principal axes, whereas stochastic modelling mainly affects the magnitude and anisotropy of positional uncertainty.

METHODOLOGY

The proposed methodology examines how the precision characteristics assigned to angular and distance observations are propagated through the least-squares adjustment process and subsequently influence the covariance

structure of the adjusted coordinates. Particular attention is paid to the resulting positional uncertainty, the geometry of the error ellipse, and the orientation of its principal axes.

The computational workflow adopted in this investigation can be summarized as:

measurement precision→weights→normal matrix→cofactor and covariance matrices→positional error→error ellipse.

To isolate the effect of stochastic modelling, the geometric configuration of the network is kept identical throughout all numerical experiments. Only the weighting scheme assigned to the observations is modified. Consequently, any variation observed in the covariance matrices or in the characteristics of the error ellipse originates exclusively from the adopted stochastic model rather than from changes in network geometry.

Observation Precision and Positional Influence

For a measured direction R over a distance D, with standard deviation m_R, the transverse positional effect is

$$m_{Transverse} = Dtan(m_R) \tag{1}$$

The standard deviation of a measured distance is represented by

$$m_D\ [mm] = a[mm] + b[\tfrac{mm}{km}].D[km], \tag{2}$$

where a is the constant instrumental component, b is the proportional component, and D is the measured distance. Consequently, distance observations mainly determine the radial component of the point position, whereas angular observations predominantly affect the transverse component. Their relative contribution depends on both the network geometry and the adopted stochastic model.

Observation Model and Weighting

For two points i and j, $\Delta X_{ij} = X_j - X_i$, $\Delta Y_{ij} = Y_j - Y_i$ and O_i denotes the orientation angle of the station i. The functional models for distance and direction observations are as follows:

$$\mathrm{D}_{ij} = \sqrt{\Delta X_{ij}{}^2 + \Delta Y_{ij}{}^2} \tag{3}$$

$$R_{ij} = atan\left(\frac{\Delta Y_{ij}}{\Delta X_{ij}}\right) - O_i \tag{4}$$

The linearized correction equations for distance and direction observations provide the corresponding rows of the design matrix, whose coefficients directed respectively along and perpendicular to the observed line are:

$$v_{ij}^D = \alpha_{ij}^D \delta x_i + b_{ij}^D \delta y_i + c_{ij}^D \delta x_j + d_{ij}^D \delta y_j + f_{ij}^D, \tag{5}$$

where $a_{ij}^D = -cos\alpha_{ij}^0,\ b_{ij}^D = -sin\alpha_{ij}^0,\ c_{ij}^D = -a_{ij}^D, d_{ij}^D = -b_{ij}^D$ and $f_{ij}^D = D_{ij}^0 - D_{ij}'$;

$$v_{ij}^R = \alpha_{ij}^R \delta x_i + b_{ij}^R \delta y_i + c_{ij}^R \delta x_j + d_{ij}^R \delta y_j - \delta O_i + f_{ij}^R \tag{6}$$

where $a_{ij}^R = \frac{\Delta Y_{ij}^0}{\left(D_{ij}^0\right)^2}\rho^{cc}$, $b_{ij}^R = -\frac{\Delta X_{ij}^0}{\left(D_{ij}^0\right)^2}\rho^{cc}$, $c_{ij}^R = -\frac{\Delta Y_{ij}^0}{\left(D_{ij}^0\right)^2}\rho^{cc}$, $d_{ij}^R = \frac{\Delta X_{ij}^0}{\left(D_{ij}^0\right)^2}\rho^{cc}$ and

$$f_{ij}^R = arctg\left(\frac{Y_j^0 - Y_i^0}{X_j^0 - X_i^0}\right) - O_i^0 - R_{ij}'$$

With zero indices are given the approximate values calculated and with primes – the observed ones.

Two alternative weighting models are considered to evaluate also the influence of centering errors on the covariance structure and the resulting error ellipse.

Case 1: Equal weights of directions without explicit centering errors

In the first case, all measured directions are assumed to have the same a priori standard deviation m_0^R. The centering errors of the instrument and the observed signals are not introduced separately and are assumed to be implicitly included in the adopted constant directional accuracy. Therefore, $\mathrm{m}_{\mathrm{ij}}^R = \mathrm{m}_0^R$ and all directions receive equal weights:

$$p_{ij}^R = \frac{\left(\mathrm{m}_0^R\right)^2}{\left(\mathrm{m}_0^R\right)^2} = 1 \tag{7}$$

For the distance observations, only the standard deviation of the measured distance is considered to be calculated by Eq. (2). The corresponding weight is

$$p_{ij}^{D} = \frac{\left(\mathrm{m}_0^R\right)^2}{\left(\mathrm{m}_{\mathrm{ij}}^D\right)^2} \tag{8}$$

This model provides a reference solution in which all directions have equal stochastic significance, whereas the distance weights depend only on the nominal distance-measurement precision.

Case 2: Individual weights including instrument and signal centering errors

In the second model, the variance of each direction and distance observation is determined individually. Instrument- and signal-centering errors are explicitly included.

For a direction measured over a sight length D_{ij}, the centering errors produce additional transverse positional components. Their equivalent angular contribution is obtained by adding the centering components and dividing the total transverse centering error by the sight length. The total variance of direction R_{ij} is therefore:

$$\mathrm{m}_{ij}^R = \sqrt{\mathrm{m}_0^{R\,2} + \left(\frac{m_{cen.instr.} + m_{cen.sign.}}{\mathrm{D}_{ij}}\rho^{cc}\right)^2} \tag{9}$$

where:

m_0^R is the standard deviation of the direction measurement (in some cases it can be the sum of the pointing and reading errors);

$m_{cen.instr.}$ is the transverse component of the instrument-centering error relative to sight;

$m_{cen.sign.}$ is the transverse component of the signal-centering error;

D_{ij} is the sight length;

ρ is the conversion factor corresponding to the adopted angular unit.

If the angular measurements and standard deviations are expressed in radians, the conversion factor is omitted.

The individual weight of direction R_{ij} is then:

$$p_{ij}^{R} = \frac{\left(\mathrm{m}_0^R\right)^2}{\left(\mathrm{m}_{\mathrm{ij}}^R\right)^2} \tag{10}$$

Consequently, short directions receive lower weights when centering errors are significant, because the same linear centering error produces a larger angular effect at a shorter sight length.

For distance D_{ij}, the total variance includes the instrumental distance-measurement error and the longitudinal components of the instrument- and signal-centering errors:

$$\mathrm{m}_{ij}^D = \sqrt{\mathrm{m}_{\mathrm{ij}\,0}^{D\;2} + m_{cen.instr.}^{\;2} + m_{cen.sign.}^{\;2}} \tag{11}$$

Here $\mathrm{m}_{\mathrm{ij}\,0}^{D}$ is the nominal standard deviation of the distance observation calculated by Eq. (2). The corresponding individual weight of distance D_{ij} is then:

$$p_{ij}^{D} = \frac{\left(\mathrm{m}_0^R\right)^2}{\left(\mathrm{m}_{ij}^D\right)^2} \tag{12}$$

The comparison between the two models shows how the explicit inclusion of centering errors alters the relative contributions of individual observations. These changes propagate into the coordinate variances and covariances and may affect the mean square positional error, the lengths of the error-ellipse axes, and its orientation.

Accordingly, the weight matrix for the first stochastic model is

$$P^{(1)} = \mathrm{diag}\left(1, \ldots, 1, \frac{\left(\mathrm{m}_0^R\right)^2}{\left(\mathrm{m}_1^D\right)^2}, \ldots, \frac{\left(\mathrm{m}_0^R\right)^2}{\left(\mathrm{m}_{n_D}^D\right)^2}\right) \tag{13}$$

whereas the weight matrix for the second model is

$$P^{(2)} = \mathrm{diag}\left(\frac{\left(\mathrm{m}_0^R\right)^2}{\left(\mathrm{m}_1^R\right)^2}, \ldots, \frac{\left(\mathrm{m}_0^R\right)^2}{\left(\mathrm{m}_{n_R}^R\right)^2}, \frac{\left(\mathrm{m}_0^R\right)^2}{\left(\mathrm{m}_1^D\right)^2}, \ldots, \frac{\left(\mathrm{m}_0^R\right)^2}{\left(\mathrm{m}_{n_D}^D\right)^2}\right) \tag{14}$$

The comparison of the two models quantifies the influence of explicitly introducing centering errors. The resulting changes in observation weights propagate through the normal equations and modify the coordinate variances and covariances, the error-ellipse axes, and potentially its orientation.

Methodological note: The weights in Eqs. (7)-(14) are relative weights normalized with respect to the reference directional variance. This formulation is valid when the angular and linearized distance equations are expressed in consistent units. Alternatively, the weight matrix may be formed directly from the inverse observation variances.

Covariance Propagation and Error Ellipse

The linearized observation model is written as $v = A\delta x + f$ where v is the vector of residuals, A is the design matrix, δx is the vector of unknown corrections, and f is the vector of misclosures. If each part of this matrix equation is multiplied on the left with $A^T P$, then $A^T Pv = 0$ is the least-squares adjustment condition, $A^T PA = N$ is the normal matrix and $N\delta x + F = 0$ are the normal equations, where $A^T Pf = F$. The inverse of N gives the cofactor matrix

$$Q = (A^T PA)^{-1} = N^{-1} \tag{15}$$

The covariance matrix of the adjusted coordinates is

$$K = \mu^2 Q, \tag{16}$$

where μ is the a posteriori standard deviation of unit weight.

For each analysed point i, the covariance submatrix

$$K_i = \mu^2 \begin{bmatrix} Q_{XX} & Q_{XY} \\ Q_{XY} & Q_{YY} \end{bmatrix} = \begin{bmatrix} {\sigma_{XX}}^2 & \sigma_{XY} \\ \sigma_{XY} & {\sigma_Y}^2 \end{bmatrix} \tag{17}$$

is used to determine the coordinate standard deviations and the mean square positional error:

$m_X = \sigma_{XX} = \mu\sqrt{Q_{XX}}$, $m_Y = \sigma_{YY} = \mu\sqrt{Q_{YY}}$ and $m_P = \sqrt{{m_X}^2 + {m_Y}^2} = \sqrt{{\sigma_{XX}}^2 + {\sigma_{YY}}^2} = \mu\sqrt{{Q_{XX}}^2 + {Q_{YY}}^2}$

The principal characteristics of the error ellipse are obtained from the eigenvalues of the cofactor or the covariance matrix. Although m_P characterizes the overall positional accuracy, it does not describe the directional distribution of the uncertainty. For this purpose, the eigenvalues and eigenvectors of the covariance submatrix are determined.

The eigenvalues are

$$\lambda_{\{1,2\}} = \frac{tr(Q) \pm \sqrt{tr(Q)^2 - 4\det(Q)}}{2}, \tag{18}$$

where $tr(Q) = Q_{XX} + Q_{YY}$ and $\det(Q) = Q_{XX}Q_{YY} - Q_{XY}^2$.

The semi-major and semi-minor axes of the standard error ellipse are:

$a = \mu\sqrt{\lambda_1}$ and $b = \mu\sqrt{\lambda_2}$ (when $\lambda_1 \geq \lambda_2$).

The orientation of the major axis is determined by

$$\alpha = \frac{1}{2} atan\left(\frac{2Q_{XY}}{Q_{XX} - Q_{YY}}\right) \tag{19}$$

The eigenvectors associated with λ_1 and λ_2 define the direction of maximum and minimum dispersion.

For further visualization and analysis, the covariance matrix is transformed into its principal coordinate system by translating the origin to the adjusted point coordinates and rotating the coordinate axes through the angle calculated for the orientation of the error ellipse. This transformation is expressed as:

$$\begin{pmatrix} x' \\ y' \end{pmatrix} = \begin{pmatrix} \cos\alpha & \sin\alpha \\ -\sin\alpha & \cos\alpha \end{pmatrix} \begin{pmatrix} X - M(X) \\ Y - M(Y) \end{pmatrix} \tag{20}$$

$M(X)$ and $M(Y)$ are the adjusted coordinates of the analyzed point. After the transformation, the main axes of the error ellipse are aligned with the transformed coordinate axes x' and y'. Consequently, the covariance matrix becomes diagonal, while the transformed coordinate variances correspond directly to the variances along the semi-major and semi-minor axes.

The orientation angle derived from Eq. (19) specifies the direction of the semi-major axis, which corresponds to the maximum positional uncertainty. Conversely, the eigenvector associated with the smaller eigenvalue defines the direction of minimum positional uncertainty. Consequently, eigenvalue decomposition provides a complete description of the error ellipse by simultaneously determining its size, shape and orientation.

Because the covariance matrix depends on the adopted stochastic model, modifying the observation weights changes the covariance structure of the adjusted coordinates. These changes are reflected mainly in the coordinate variances and, to a lesser extent, in the covariance term. As demonstrated in the subsequent numerical analyses, realistic variations in observation weighting influence primarily the dimensions and eccentricity of the error ellipse, whereas its orientation remains almost unchanged except in situations where the eigenvalues become nearly identical.

The semi-major and semi-minor axes obtained from Eq. (18) define the standard error ellipse. For any prescribed confidence level, the corresponding confidence ellipse is obtained by scaling both axes with the appropriate coverage

factor k. Since the same scaling coefficient is applied to each principal axis, the orientation of the ellipse is preserved while only its size changes.

The confidence ellipse preserves the same orientation as the standard error ellipse, while only its dimensions are scaled according to the selected confidence level. Since the objective of the present study is to compare weighting strategies, the standard error ellipse is used throughout the numerical analysis because it reflects the covariance characteristics of the adjusted coordinates.

Algorithmic Optimization Procedure

The proposed methodology is implemented as an iterative computational algorithm in which alternative stochastic models are analyzed while the geometric configuration of the network remains unchanged.

For every weighting strategy, the following sequence of calculations is performed:

1. Construction of the design matrix from the linearized observation equations;
2. Formation of the weight matrix for the observation according to the adopted stochastic model;
3. Computation of the normal equations and determination of the cofactor matrix;
4. Estimation of the covariance matrix of the adjusted coordinates;
5. Extraction of the covariance submatrix for each analyzed point;
6. Determination of the eigenvalues and eigenvectors;
7. Computation of the semi-major axis, semi-minor axis and orientation angle of the corresponding error ellipse;
8. Comparison of the obtained positional accuracy indicators for the investigated weighting strategies.

The computational chain may therefore be summarized as:

$$(m_R, m_D) \rightarrow P \rightarrow N \rightarrow Q \rightarrow K \rightarrow (M_P, a, b, \alpha),$$

where the observation precisions define the weighting matrix, the weighting matrix determines the covariance characteristics of the adjusted coordinates, and these covariance characteristics determine the dimensions and orientation of the error ellipse.

This algorithm enables different stochastic models to be evaluated quantitatively while excluding the influence of network geometry. Consequently, the effect of angular and distance observation weights on the direction of maximum dispersion can be analyzed independently, providing a practical basis for selecting an appropriate observation strategy in accordance with predefined positional and directional accuracy requirements.

RESULTS AND DISCUSSION

Experimental Design

The proposed methodology was evaluated using two planar geodetic networks with different geometric characteristics and levels of complexity. The first network (Fig. 1a) represents a compact test configuration for isolating the influence of the stochastic model under controlled geometric conditions. The second network (Fig. 1b) corresponds to another (larger) surveying configuration used to verify the observed relationships under more realistic observation geometry. Throughout all experiments, the network configuration, observation scheme and approximate coordinates remained unchanged, while only the stochastic model was modified. Consequently, the observed changes in positional uncertainty can be attributed exclusively to variations in observation weighting rather than to geometric effects.

For the experimental analysis, the influence of four stochastic parameters was considered: the standard deviation of horizontal directions, the standard deviation of distance observations, the instrument centering error and the signal/target centering error (Table 1). The influence of all the parameters was evaluated through the resulting cofactor and covariance matrices, the positional standard error and the elements of the corresponding error ellipses.

Table 1 summarizes the characteristics of the investigated networks and the stochastic models taken into consideration in the experimental analysis. The network geometry and the observation configuration were kept unchanged for all experiments, while only the stochastic model was varied. Since the covariance matrix is related to the cofactor matrix by

$$K = \mu^2 Q \tag{21}$$

The comparison of the investigated stochastic models was based primarily on the cofactor matrices rather than the covariance matrices. This approach isolates the effect of observation weighting from that of the posterior variance factor and therefore provides a more objective basis for evaluating changes in positional uncertainty.

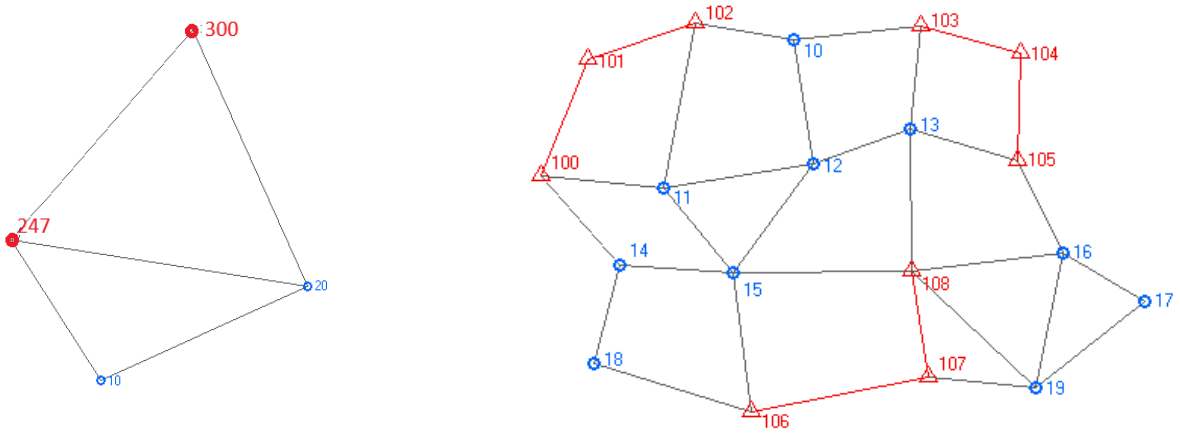

(a) (b)

FIGURE 1. Small and large test planar geodetic networks

TABLE 1. Characteristics of the investigated test networks and analysed stochastic parameters

Network	Control points	Unknown points	Total points	Average line length (m)	Investigated stochastic parameters
Small test network	2	2	4	≈48.9	m_R = 5, 10, 20 ^{cc}; m_D = 2+1D, 5+2D, 10+5D mm; m_{ci} = 2, 5 mm; m_{cs} = 2, 5 mm
Large test network	9	10	19	≈191	m_R = 10, 20 ^{cc} m_D = 2+1D, 5+2D, 10+5D mm; m_{ci} = 2 mm; m_{cs} = 2, 5 mm

Small Test Network

The compact network was used to investigate the isolated influence of the stochastic model on the precision characteristics of individual points. Owing to the fixed network geometry and the small number of unknown parameters, even minor modifications of the stochastic model can be directly related to the resulting changes in the local covariance structure.

The performed experiments show that the adopted stochastic model primarily affects the magnitude of positional uncertainty, whereas the orientation of the principal axes remains almost unchanged. Increasing the standard deviation of the angular observations leads to a systematic enlargement of the error ellipses, while deterioration of the distance precision produces a smaller but still noticeable increase in their dimensions. In contrast, increasing the centering errors from 2 mm to 5 mm produces only minor changes in both the positional precision and the ellipse parameters.

TABLE 2. Qualitative influence of the investigated stochastic parameters in the small test network

Investigated parameter	Influence on positional precision	Influence on ellipse orientation
Direction standard deviation	Strong	Negligible
Distance standard deviation	Moderate	Negligible
Instrument centering error	Small	Negligible
Target centering error	Small	Negligible

Although both unknown points were adjusted using the same observation configuration and identical stochastic parameters, their uncertainty characteristics differ noticeably. These differences confirm that local network geometry is the primary factor governing the anisotropy of positional uncertainty.

A comparison of the investigated stochastic models shows that centering errors have a substantially weaker effect than the observation precisions themselves. Introducing larger centering uncertainties slightly increases the corresponding cofactor matrices while causing only negligible variations in the orientation of the principal axes. This indicates that centering errors mainly affect the overall variance magnitude, whereas the directional pattern of positional uncertainty remains almost unchanged.

An apparent rotation of approximately 100 g was identified for several stochastic configurations. A closer examination of the associated eigenvalues demonstrates that this phenomenon does not correspond to an actual rotation of the uncertainty field. Instead, it occurs when the two eigenvalues become nearly identical and the error ellipse approaches a circular shape. In such situations, the numerical exchange of the principal axes produces an apparent change in orientation, although the spatial distribution of positional uncertainty is essentially preserved.

Overall, the results obtained from the compact network confirm that the orientation of the error ellipse is governed primarily by the network geometry, whereas its dimensions and eccentricity are influenced mainly by the adopted stochastic model. Therefore, optimization efforts should concentrate on reducing positional uncertainty, while recognizing that the direction of maximum dispersion is controlled largely by the network layout.

For the small test network, increasing the standard deviation of horizontal directions from 5 to 20 cc increased the mean positional error, the semi-major axis, and the semi-minor axis by approximately 132%, 108%, and 262%, respectively, whereas the mean ellipse axis ratio decreased by approximately 40%. Increasing the nominal distance uncertainty from 2+1D to 5+2D resulted in reductions of approximately 42%, 37%, and 56% in the corresponding absolute uncertainty measures, while the mean axis ratio increased by approximately 36%. This behavior is attributed to differences in the estimated posterior variance factors and should not be interpreted as evidence that lower-precision distance observations improve network quality.

Large Test Network

The large test network was introduced to assess whether the findings identified in the small test network remain valid under different and more realistic surveying conditions. Unlike the first example, the larger network contains ten unknown points distributed over a considerably larger area and therefore exhibits a more heterogeneous precision distribution. Three representative stochastic models were analyzed, corresponding to different combinations of angular precision, distance precision and centering errors. The reported values include the coordinate standard deviations, the positional standard error and the semi-major and semi-minor axes of the corresponding error ellipses.

Since the covariance matrix is proportional to the product of the cofactor matrix and the posterior variance factor, a reduction of the latter compensates for the deterioration of the assumed distance precision and results in smaller covariance ellipses. Consequently, direct comparison of covariance matrices alone may lead to misleading conclusions regarding the quality of different stochastic models.

The spatial distribution of uncertainty remained consistent throughout all experiments. These observations remained practically unchanged despite the modifications of the stochastic model, confirming that the ranking of point precision is dependent primarily on network geometry.

The orientation of the principal axes showed only negligible changes between the investigated stochastic models. Small numerical differences were observed only for points with nearly equal eigenvalues, where the error ellipse approaches a circular shape. Under these conditions, the reported direction angle of the major axis may change abruptly owing to the interchange of the eigenvectors rather than to a physical rotation of the area of uncertainty. The direction of maximum dispersion should be interpreted together with the corresponding eigenvalues and ellipse eccentricity rather than solely through its reported orientation.

Overall, the results obtained from the large network confirm the observations derived from the compact test network. The adopted stochastic model primarily affects the magnitude of coordinate uncertainty. In contrast, the spatial distribution of precision and the orientation of the error ellipse axes remain predominantly defined by the network geometry.

In the large test network, the increase in the standard deviation of horizontal directions from 10 cc to 20 cc was accompanied by increases of approximately 28%, 23%, and 36% in the mean positional error, semi-major axis, and semi-minor axis, respectively, while the mean ellipse axis ratio decreased by about 11%. Increasing the nominal distance uncertainty from 2+1D to 10+5D resulted in decreases of approximately 24%, 22%, and 27% in the

corresponding absolute uncertainty measures, whereas the mean axis ratio increased by approximately 10%. These changes reflect the combined influence of the stochastic model and the posterior variance factor.

DISCUSSIONS

The results obtained from the two planar geodetic networks provide a consistent basis for separating the effects of the stochastic model from those of the network geometry. Although modifications to the stochastic assumptions noticeably influence the estimated coordinate precision, they have only a limited impact on the orientation of the principal axes of the error ellipses. The numerical analyses consistently show that increasing the uncertainty of horizontal direction observations reduces positional accuracy, whereas changes in the stochastic characteristics of distance measurements primarily influence the dimensions and eccentricity of the ellipses. Consequently, the orientation of the maximum dispersion direction appears to be controlled mainly by the geometric configuration of the network, while the stochastic model determines the overall level and directional distribution of positional uncertainty.

The influence of observation weighting is expressed predominantly through changes in the eigenvalues of the covariance matrix, which directly affect the lengths of the principal axes and the shape of the error ellipse. Variations in the orientation angle become noticeable only when both eigenvalues converge to nearly identical values, producing an almost circular ellipse. Under these conditions, the apparent rotation results from the mathematical exchange of the principal axes during eigenvalue decomposition rather than from an actual modification of the uncertainty field.

Another important outcome of this investigation is the different role played by the cofactor and covariance matrices in stochastic analysis. Because covariance matrices contain the estimated posterior variance factor, their direct comparison may obscure the real influence of alternative stochastic models. Cofactor matrices, on the other hand, depend exclusively on the adopted observation weights and therefore provide a more reliable basis for evaluating how changes in the stochastic model affect positional uncertainty and the direction associated with maximum dispersion.

The agreement of the results obtained from both test networks demonstrates that these observations are not restricted to a particular network size or configuration. Instead, they reflect general characteristics of least-squares adjustment and covariance propagation. The present investigation therefore complements the conventional interpretation of error ellipses by showing that realistic modifications of the stochastic model mainly alter the magnitude and anisotropic behavior of positional uncertainty, whereas the orientation of the principal uncertainty direction remains largely unaffected. From a practical perspective, these findings support the selection of appropriate stochastic models during the design, adjustment, and quality assessment of planar geodetic networks.

CONCLUSIONS

This study examined how different stochastic models influence the covariance structure of adjusted coordinates and the directional properties of positional uncertainty in combined angular–distance geodetic networks. An integrated computational approach was developed by combining least-squares adjustment, stochastic modelling, covariance propagation and eigenvalue analysis, allowing alternative observation-weighting strategies to be evaluated within a common analytical framework.

The performed numerical analyses confirmed that modifying the observation weights primarily changes the covariance characteristics of the adjusted solution, which is reflected in the size and shape of the corresponding error ellipses. In contrast, the orientation of the principal axes remains largely controlled by the geometric configuration of the network and exhibits only limited sensitivity to realistic changes in the stochastic model.

The inclusion of instrument- and signal-centering errors provides a more representative stochastic description of the measurement process and leads to covariance estimates that better reflect actual observation conditions. Consequently, the proposed methodology enables a more reliable assessment of positional uncertainty without altering the underlying network geometry.

The presented approach offers practical support for the design and adjustment of planar geodetic networks by facilitating the evaluation of different observation-weighting strategies. It may also assist surveyors in selecting stochastic models that satisfy both positional and directional accuracy requirements for specific engineering applications.

REFERENCES

1. V. I. Peevski, Adjustment by the Method of Least Squares, 3rd ed. (Technika Publishing House, Sofia, 1973), pp. 387–391.
2. M. M. Mashimov, Adjustment of Geodetic Networks (Nedra Publishing House, Moscow, 1979), pp. 205–207.
3. P. Tomova-Hincheva, P. M. Bakanov, K. N. Kostadinov, B. P. Banov, and V. G. Valchinov, Exercises in the Theory of Mathematical Processing of Geodetic Measurements (University of Architecture, Civil Engineering and Geodesy, Sofia, 1986), pp. 273–276.
4. K. N. Kostadinov and V. G. Valchinov, Mathematical Processing of Geodetic Measurements (University of Architecture, Civil Engineering and Geodesy, Sofia, 2012), pp. 287–294.
5. R. E. Deakin, "The Standard Error Ellipse," in Notes on Least Squares (RMIT University, Melbourne, 2005), Chap. 8, pp. 8-1–8-10.
6. V. A. Gordeev and G. G. Shevshenko, "Identification of an Ellipse and a Sub-Ellipse of Errors by Elements of the Covariance Matrix," Geodesy 1007(5), 2–10 (2024), DOI: 10.22389/0016-7126-2024-1007-5-2-10.
7. P. D. Penev, Engineering Geodesy 2: Geodetic Methods for Monitoring Engineering Structures (University of Architecture, Civil Engineering and Geodesy, Sofia, 2025).
8. A. Angelov, "Precise Geodetic Setting Out Activities in the Construction of Engineering Structures with Orientation in Predetermined Direction," Inżynieria Mineralna – Journal of the Polish Mineral Engineering Society 53(1), 369–377 (2024), DOI: 10.29227/IM-2024-01-42.
9. A. A. Stefanova, "Location Selection Method for the Initial Points of Horizontal Bridge Geodetic Networks," in MATTECH 2024 Conference Proceedings, Vol. 2, Section Geodesy, Cartography and Cadastre, pp. 289–297 (2024), DOI: 10.46687/MOIB2093.
10. S.-L. Kuang, "Optimization and Design of Deformation Monitoring Schemes," Ph.D. thesis, Department of Surveying Engineering, University of New Brunswick, Fredericton, Canada, Technical Report No. 157, 1991.
11. R. A. Ivanov, Engineering Surveying and Deformation Surveys, 1st ed. (Higher School of Transport "Todor Kableshkov," Sofia, 2020), ISBN 978-954-12-0272-2.
12. R. A. Ivanov, C. Mickrenska-Cherneva, and N. I. Babunska-Ivanova, "Deformation Monitoring Surveys of Roads and Railways," in 2024 Mediterranean Smart Cities Conference (MSCC) (IEEE, Martil, Morocco, 2024), DOI: 10.1109/MSCC62288.2024.10697034.